Biosensors and Bioelectronics 64 (2015) 469–476

Contents lists available at ScienceDirect

Biosensors and Bioelectronics

journal homepage: www.elsevier.com/locate/bios

# Real-time QCM-D monitoring of cancer cell death early events in a dynamic context

Laetitia Nowacki [a,b,1], Julie Follet [b,1], Muriel Vayssade [b], Pascale Vigneron [b], Laura Rotellini [b], Florian Cambay [b], Christophe Egles [b,c,*], Claire Rossi [a,**]

[a] FRE CNRS 3580, Génie Enzymatique et Cellulaire, Université de Technologie de Compiègne, Centre de Recherches de Royallieu, CS 60319, 60203 Compiègne, France

[b] UMR CNRS 7338, BioMécanique et BioIngénierie, Université de Technologie de Compiègne, Centre de Recherches de Royallieu, CS 60319, 60203 Compiègne, France

[c] Department of Oral and Maxillofacial Pathology, Tufts University, School of Dental Medicine, 1 Kneeland St, Boston, MA 02111, United States

ARTICLE INFO

*Article history:*
Received 31 July 2014
Received in revised form
18 September 2014
Accepted 23 September 2014
Available online 26 September 2014

*Keywords:*
Quartz crystal microbalance with dissipation
Whole cell biosensor
Human breast cancer cell line MCF-7
Staurosporine
Apoptosis
Morphology dynamic measurement

ABSTRACT

Since a few years, the acoustic sensing of whole cell is the focus of increasing interest for monitoring the cytoskeletal cellular response to morphological modulators. We aimed at illustrating the potentialities of the quartz crystal microbalance with dissipation (QCM-D) technique for the real-time detection of the earliest morphological changes that occur at the cell-substrate interface during programmed cell death. Human breast cancer cells (MCF-7) grown on serum protein-coated gold sensors were placed in dynamic conditions under a continuous medium flow. The mass and viscoelasticity changes of the cells were tracked by monitoring the frequency and dissipation shifts during the first 4 h of cell exposure to staurosporine, a well-known apoptosis inducer. We have identified a QCM-D signature characteristic of morphological modifications and cell detachment from the sensing surface that are related to the pro-apoptotic treatment. In particular, for low staurosporine doses below 1 μM, we showed that recording the dissipation shift allows to detect an early cell response which is undetectable after the same duration by the classical analytical techniques in cell biology. Furthermore, this sensing method allows quantifying the efficiency of the drug effect in less than 4 h without requiring labeling and without interfering in the system, thus preventing any loss of information. In the actual context of targeted cancer therapy development, we believe that these results bring new insights in favor of the use of the non invasive QCM-D technique for quickly probing the cancer cell sensitivity to death inducer drugs.

© Elsevier B.V. All rights reserved.

## 1. Introduction

Over the last few years, the increasing number of scientific reports concerning the use of the acoustic biosensors and more particularly the quartz crystal microbalance (QCM) technique for whole cell monitoring has stressed the growing interest for this technology. Contrary to the cellular impedance biosensors also used to detect morphological cell responses in real time, the QCM detection is restricted to the modifications occurring in the cell–substrate interaction and do not take into account the cell–cell contacts (Asphahani and Zhang, 2007; Wegener et al., 2001). For this reason, piezoelectric mass-sensing was first widely applied to study various aspects of cell–surface interactions as attachment, adhesion and spreading (Chen et al., 2012; Cooper and Singleton, 2007; Saitakis and Gizeli, 2012; Wegener et al., 2001; Zhou et al., 2012b). More recently the acoustic sensors were used to study the effect of modulators of the morphological and cytoskeletal cellular response (Braunhut et al., 2005; Fatisson et al., 2011; Marx et al., 2007; Tymchenko et al., 2012; Zhou et al., 2012a, 2012c).

The QCM technique is a highly sensitive technique that records the frequency changes ($\Delta f$) of an oscillating piezoelectric quartz crystal to measure mass. The QCM with dissipation (QCM-D) technique presents an advantage compared to the conventional

*Abbreviations:* QCM-D, quartz crystal microbalance with dissipation; STS, staurosporine; DMSO, dimethylsulfoxide; FBS, fetal bovine serum

* Corresponding author at: UMR CNRS 7338, BioMécanique et BioIngénierie, Université de Technologie de Compiègne, Centre de Recherches de Royallieu, CS 60319, 60203 Compiègne, France. Fax: +33 3 44 20 39 10.

** Corresponding author at: FRE CNRS 3580, Génie Enzymatique et Cellulaire, Université de Technologie de Compiègne, Centre de Recherches de Royallieu, CS 60319, 60203 Compiègne, France. Fax: +33 3 44 20 39 10.

*E-mail addresses:* christophe.egles@utc.fr (C. Egles), claire.rossi@utc.fr (C. Rossi).

[1] Both authors contributed equally to this work.

http://dx.doi.org/10.1016/j.bios.2014.09.065
0956-5663/© Elsevier B.V. All rights reserved.

QCM. In addition to frequency changes, it records simultaneously the energy dissipation factor ($\Delta D$), related to the viscoelastic properties of the material adsorbed to the sensing surface. It was proved that the QCM-D is a non invasive technique for mammalian cells when the shear oscillation amplitudes smaller is 1 nm (Heitmann and Wegener, 2007). The maximum frequency penetration depth is on the order of 250 nm in water and decreases when viscoelastic material is adsorbed on the surface (Kanazawa and Gordon, 1985). Consequently, in whole cell sensing, the probing wave never exceeds the middle of the cell (Dixon, 2008). Despite that, the QCM-D technique appears to be particularly well suited for real-time acquisition of cell responses without requiring labeling and without interfering with the system, thus preventing any loss of information (Fatisson et al., 2011; Tymchenko et al., 2012; Watarai et al., 2012).

Given those advantages, this technology could prove to be very powerful when applied to cell death monitoring in response of cytotoxic agent exposure as it allows recording in a timely manner the reaction of the cell. Cell death engagement is a complex process that implies a plethora of mechanisms, which led to the classification of specific cell death subtypes in response to typical internal and/or external signals. Assessing the particular cell death pathway involved in the studied context requires the setting of different techniques, such as electron, fluorescence or light microscopy or flow cytometry (Kepp et al., 2011; Galluzzi et al., 2012). Most of the time, these techniques are time- and money-consuming and require cell handling, which could induce some loss of information (Archana et al., 2014; Demchenko, 2012). The QCM-D offers the possibility of an easy *in-situ* determination of the global cellular response induced by cytotoxic agents in real time. Few recent articles have already established that a correlation exists between the $\Delta f$ and $\Delta D$ profiles and the type of cell death process (Braunhut et al., 2005; Fatisson et al., 2011; Marx et al., 2007; Tymchenko et al., 2012). The point stresses the interest to extend the QCM-D use to fast and reliable cytotoxic molecule screening.

To date, published examples of cell response monitoring based on QCM-D sensor are rare, in particular with cells placed under a continuous medium flow, while a dynamic system better mimics the physiological context (Fatisson et al., 2011; Tymchenko et al., 2012). There is a real need to acquire more data on QCM-D monitoring of cell death processes in order to better link the first global cell–surface interaction changes with the type of cell response. In this article, we have explored if the ability of the QCM-D technology to detect viscoelastic changes can bring new insight about the first modifications to cell-substrate interaction that are related to a cell death process. We examined the effect of the staurosporine (STS), a protein kinase inhibitor known to induce the apoptosis, on the human breast cancer cell line MCF-7 (Mooney et al., 2002; Tamaoki et al., 1986; Xue et al., 2003). The frequency and dissipation recording by QCM-D was completed by a direct observation of the cells using a polarized light microscopy. This work paves the road to real-time, rapid and cost-effective screening of anticancer drug candidates by the QCM-D technique.

## 2. Materials and methods

### 2.1. Reagents

STS and dimethyl sulfoxide (DMSO) were supplied by Sigma-Aldrich. A stock solution of STS was prepared in DMSO at 214 μM. Further dilutions of this stock solution into the cell culture medium were carried out to the desired concentrations. Phosphate Buffer Saline solution (PBS) (sodium chloride 0.13 M, potassium chloride 2.7 mM, disodium phosphate 8 mM, potassium phosphate 1.5 mM at pH 7.4) was filtered (0.22 μM) and autoclaved. Water was deionized (resistivity $> 18.2\ \mathrm{m\Omega\ cm^{-1}}$) and filtered using a MilliQ plus unit (Merk-Millipore), degassed and autoclaved. All chemical were analytical grade reagents.

### 2.2. Cell culture

The human breast adenocarcinoma cell line MCF-7 (ATCC: HTB-22) was cultured at 37 °C with 5% $CO_2$ in 75 $cm^2$ flasks (Falcon) and maintained in modified Eagle's medium (MEM, Invitrogen) supplemented with 10% (v/v) heat-inactivated fetal bovine serum (FBS, Lonza), penicillin (100 U/mL, Invitrogen), streptomycin (100 μg/mL, Invitrogen) and 1% (v/v) L-glutamine (Invitrogen). This medium is called complete medium in the rest of the manuscript. For QCM-D experiments, cells were washed with PBS at 37 °C, and dissociated with 0.25% trypsin–EDTA solution (Invitrogen). The cell suspension was centrifuged 4 min at 200 g and resuspended in complete medium before deposition on the quartz crystal surface.

### 2.3. Apoptosis quantification in MCF-7 cells treated with STS

To assess apoptosis induction, MCF-7 cells were allowed to attach on tissue culture polystyrene surface for 2 h, treated with STS during 4 or 24 h and labeled with Annexin-V-FITC (Beckman Coulter). Cell culture medium was completed with DMSO at the same concentration as in the 10 μM STS solution to avoid any artifact due to DMSO. According to the manufacturer's instructions, cells were washed with PBS and suspended in the binding buffer at $5 \times 10^5$ to $5 \times 10^6$ cells/mL. 1 μL of Annexin-V FITC solution and 5 μL of propidium iodide solution were added to 100 μL of cell suspension. Cells were incubated for 15 min on ice in the dark, and then diluted by adding 400 μL of binding solution. The Annexin-V positive/propidium iodide negative cell populations were detected with a Gallios flow cytometer (Beckman Coulter) and were representative of apoptotic cells.

### 2.4. Quartz crystal microbalance with dissipation assays

The QCM-D measurements were performed with the Q-Sense E1 instrument equipped with a window module (Q-Sense, Biolin-Scientific) and gold coated quartz crystals (QSX301). Resonance frequency and dissipation shifts were simultaneously measured at the 3rd, 5th and 7th overtones and frequency shifts were normalized by division with the overtone number.

Prior to mounting, the crystals were precleaned and exposed to a UV/ozone light treatment for 10 min and then immersed in a freshly prepared solution of 5:1:1 $H_2O/H_2O_2$ (35%)/$NH_3$ (30%) at 70 °C for 5 min (Vockenroth et al., 2009). After being rinsed with ultrapure water and dried, the sensors were immersed in a penicillin (200 U/mL) and streptomycin (200 μg/mL) solution under stirring conditions during two hours to ensure the absence of contamination. The cells were seeded on the crystal as follows: crystals were equilibrated in sterile PBS prior to deposition of 250 μL of complete medium onto the gold surface (Zhou et al., 2012a). After 2 h incubation, the medium was removed and 30,000 cells in complete $CO_2$-independent medium (complete medium with 0.02 M HEPES (2-[4-(2-hydroxyethyl)piperazin-1-yl]ethanesulfonic acid, Gibco) were added on the gold surface of the sensor. Cells were allowed to attach for 24 h at 37 °C and under a 5% $CO_2$ atmosphere. For each experiment, two sensors were cell-coated in parallel. One was used for controlling the number of attached and unattached cells.

All measurements were performed at 37 °C in a flow-through mode using a peristaltic pump. The maintaining of a fixed temperature in the QCM-D chamber was controlled and recorded as a function of time. All solutions were degassed, equilibrated at

37 °C before injection in the QCM-D chamber and all media were buffered with 20 mM of HEPES at pH 7.4. The MCF-7 cell layer was equilibrated 2 h in the QCM-D chamber under a flow rate of 12 μL/min of $CO_2$-independent medium at 37 °C. The equilibration medium was completed with DMSO at the same concentration as in the STS's solution to avoid any artifact due to DMSO. Then, STS (from 10 nM to 10 μM in complete $CO_2$-independent medium) was injected at flow rate of 12 μL/min for 4 h and $\Delta f$ and $\Delta D$ evolution were recorded. At the end of the experiment, the sensor was removed and residual cells were trypsinized and counted, as well as the cells recovered in the collector to the chamber outlet.

### 2.5. Microscopic observations

Simultaneously with recordings of frequency and dissipation, cell morphology modifications were monitored by polarized light microscopy with a Leitz Orthoplan in reflection mode equipped with a 10 ×, NPL / 0.2 P objective, and a Sony CCV, XCD-U100CR camera through the glass windows of the QCM-D module. The design of the experimental system used to evaluate the cell response was shown in the supplemental Fig. S1. The selected imaged area was as close as possible to the middle of the sensor surface, where the sensitivity is the highest.

For the cell imaging, the cells were seeded as described for QCM experiments and morphology was examined 24 h after seeding. MCF-7 cells were fixed with 4% paraformaldehyde for 20 min at room temperature, and then washed twice with PBS. After 15 min of permeabilization in a 0.1% Triton X-100 solution and two washes in PBS, cells were incubated in 2% bovine serum albumin solution (Sigma-Aldrich) for 1 h at room temperature. Cells were then incubated in the dark for 1 hour at room temperature with a cytoskeleton staining solution containing phalloidin 5 U/mL (phalloidin-X5, Fluoprobes) and DAPI (4′,6′-diamidino-2-phenylindole, 1 μg/mL, Sigma-Aldrich) for nuclear staining in PBS. After three washes in PBS, cells were mounted in Mowiol (Sigma-Aldrich) and observed with a fluorescence microscope (DMI600, Leica System).

MCF-7 cell morphology was also examined using scanning electron microscopy. Glass round coverslips (14 mm of diameter) were coated with 2 nm of chromium and 47 nm of gold by thermal evaporation as previously described (Rossi et al., 2007). The gold layer thickness was identical to the one on the quartz crystal. Theses surfaces were cleaned and protein-coated according the same procedure as for quartz crystal. Cells were allowed to attach on these FBS-protein-coated gold surfaces and cultured for 4 h with different STS concentrations (10 nM, 1 μM and 10 μM) in dynamic conditions (12 μL/min). Cells were rinsed in PBS and fixed in 3% glutaraldehyde in Rembaum buffer (pH 7.4) for 1 h. Samples were then dehydrated in a series of graded alcohols, critical-point dried from $CO_2$ (Polaron Instrument Inc.), sputter-coated with gold (Polaron) and examined in Philips scanning electron microscope (ESEM FEG XL30).

## 3. Results

The purpose of this study was to demonstrate that the early morphological changes of cancer cells, that undergo apoptosis, are detectable by QCM-D within a very short time after induction of programmed death process. Our system model was human breast cancer cells (MCF-7) grown on FBS-protein-coated gold surface. We selected the staurosporine (STS) as apoptosis inducer because its action on MCF-7 cells has been already well described (Mooney et al., 2002). We aimed at determining if a specific variation of the QCM-D signals could be related to the short-term modifications of cell-substrate interactions caused by STS in a timeframe of 4 h. In

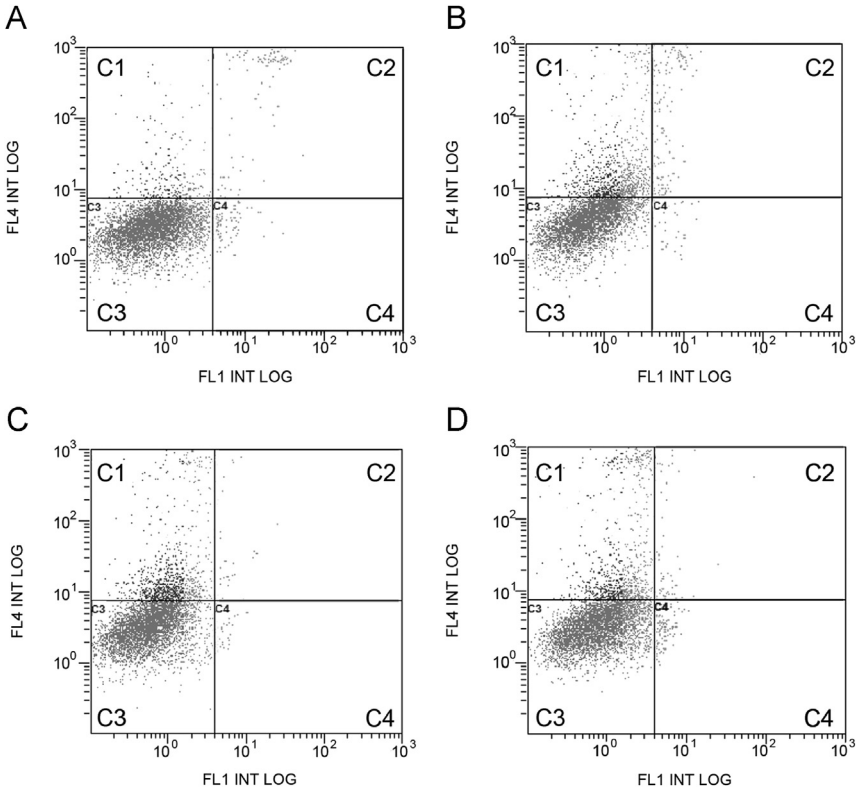


**Fig. 1.** Flow cytometry analysis of Annexin-V and propidium iodide-labeled MCF-7 cells treated for 4 h with different concentrations of STS: 0 (A); 10 nM (B); 1 μM (C) and 10 μM (D). Flow cytometry profile represents Annexin-V-FITC staining in x axis and propidium iodide staining in y axis. Dual staining of cells with Annexin-V-FITC and propidium iodide enabled categorization of cells into four regions. Region C3 shows the live cells; region C4 shows the early apoptotic cells.

addition, the real-time observation of the cell population on the gold surface during the QCM-D measurement was allowed by a glass window in the QCM-D module (Supplemental Fig. S1). To ensure reliable results, all QCM-D experiments were reproduced independently at least three times. The $\Delta f$ and $\Delta D$ curves at the 3rd overtones were displayed as the most representative of the set of experiments.

### 3.1. Detection of apoptosis induced by STS in MCF-7 cancer cells

To ensure apoptosis by STS, we first analyzed the phosphatidylserine externalization from the inner to the outer leaflet of the plasma membrane. This phenomenon is an early event during apoptotic process and is usually checked by cell labeling with Annexin-V-FITC, a protein with high affinity for phosphatidylserine. Using this common method, we investigated STS action on MCF-7 cells exposed to this drug for 4 or 24 h (Fig. 1 and Fig. S2). After 4 h exposure with different STS concentrations (0 to 10 μM), any significant effect on the percentage of apoptotic cells (Annexin-V positive/propidium iodide negative) was observed. For the highest STS dose (10 μM), this percentage remained low: 2.74% (Fig. 1.D). However the percentages of live cells (Annexin-V negative/propidium iodide negative) decreased: 91.17% in control cells, 79.21% in MCF-7 cells treated with 10 μM STS, suggesting that STS action starts to be slightly efficient from 4 h exposure. Phosphatidylserine externalization in MCF-7 cells was finally observed after 24 h treatment and was STS concentration-dependent (Fig. S2). Thus, the phosphatidylserine externalization detection allowed us to quantify apoptosis in MCF-7 cells in response to STS treatment. However this phenomenon, considered as an early event, was not detectable upon 4 h of treatment even for high STS concentration.

### 3.2. Control of the cell integrity preservation during the QCM-D measurement

Before monitoring the QCM-D signal generated by the cell reaction to the STS treatments, we first needed to ensure that the measurement design had no significant influence on the cell adhesion onto the sensor surface or on the cells themselves and as consequence on the recorded QCM-D signal.

The first step was to check if the protein coated-gold sensor used as cell culture surface could affect the cell morphology. We compared cells cultured 24 h on protein coated sensor and on polystyrene surfaces treated for cell culture, as a control surface (Fig. 2.A). The fluorescence micrographs of DAPI-stained nuclei and phalloïdin-stained actin cytoskeleton of MCF-7 cells grown as indicated above showed that the cytoskeleton architecture and the nucleus morphology features were unchanged between the both surface conditions.

During the QCM-D measurement, the cells were exposed to a continuous flow of medium and to the shear oscillations of the sensing surface. Indeed the quartz crystal microbalance with dissipation technology is based on the mechanical resonance of piezoelectric crystal quartz. As temperature and pH changes could affect the medium viscosity and the cell morphology and, as a consequence cause QCM-D signal shifts, these two parameters were strictly controlled using a QCM-D chamber thermostated at 37 °C and a buffered medium in constant renewal above the cells. In order to verify if the measurement conditions do not affect the MCF-7 layer adhesion, we controlled the stability of the signal baseline in the absence of the STS during the 4 h of frequency ($\Delta f$) and dissipation ($\Delta D$) acquisition, under a flow rate of 12 μL/min of medium at 37 °C (Fig. 2.B). In addition to the residual cell counting at the end of the 4 h of monitoring, the cells were observed throughout the QCM-D assay by using a window-equipped QCM-D module mounted in a light microscope (Fig. 2.C). The benefit of combining light microscopy with QCM-D, was to provide a real-time dual information on an identical cell population. The main limitation of this combination was the resolution of the images that was low due to the difficulty of maintaining a good focus on the same live cells during 4 h through the glass window of the QCM-D module and through the reservoir of medium under flow (Fig. S1). However, the live cell images were informative enough to allow us to correlate frequency of dissipation shift events with cell

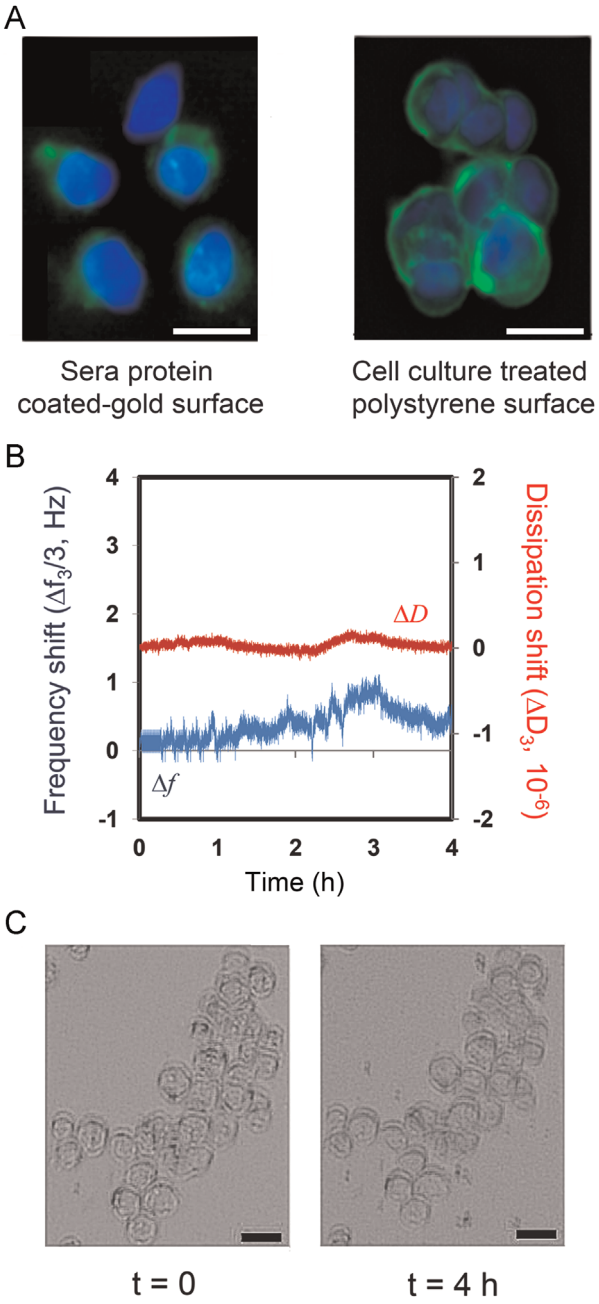


**Fig. 2.** (A) Fluorescence micrographs of DAPI-stained nuclei and phalloïdin-stained actin cytoskeleton of MCF-7 cells grown 24 h on sera protein coated-gold sensor (left) and on cell culture polystyrene (right). (B) Control of the frequency ($\Delta f$) and dissipation ($\Delta D$) baseline stability over the 4 h of monitoring the MCF-7 cell behavior while submitted to medium at a flow rate of 12 μL/min after 2 h of equilibration at the same flow rate. (C) Live images of the MCF-7 cells on the sensor surface mounted in the QCM-D chamber at the beginning (left) and at the end (right) of these 4 h of monitoring. Scale bar = 10 μm.

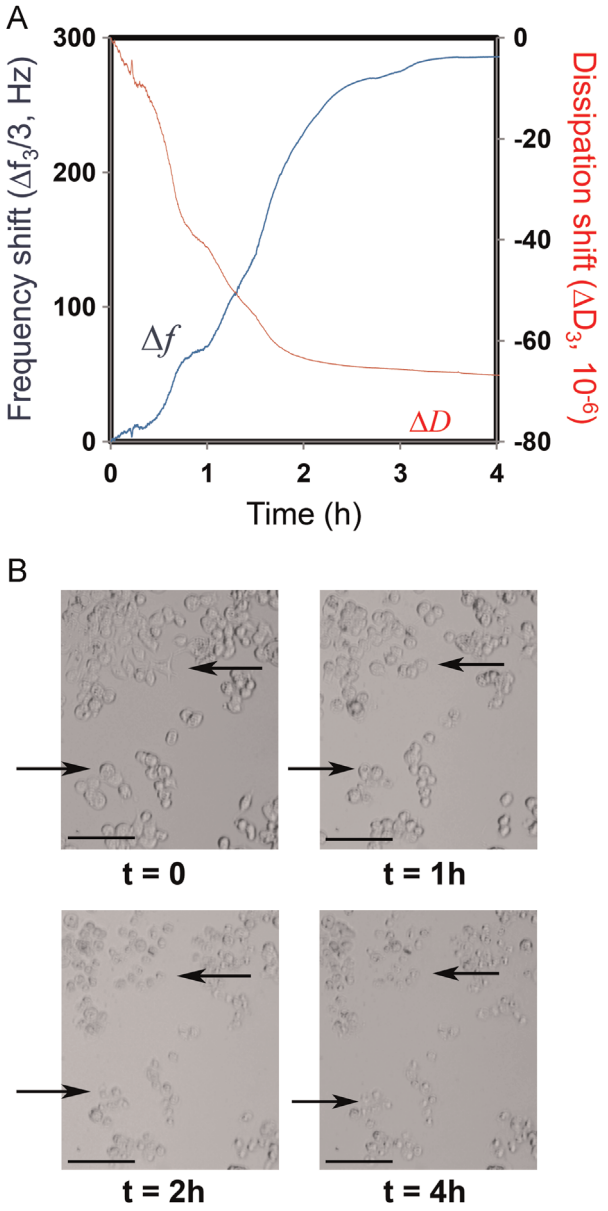


**Fig. 3.** (A) Real time QCM-D measurement of the $\Delta f$ and $\Delta D$ responses of MCF-7 cells to STS at 10 μM at 37 °C. After 2 h of equilibration in the QCM-D chamber, the MCF-7 cells were exposed during 4 h to medium containing STS at a flow rate of 12 μL/min. (B) Live images of the MCF-7 cells on the sensor surface mounted in the QCM-D chamber just before STS injection and after 1, 2 and 4 h of STS treatment. Arrows indicate the rounding-up of the cells and their detachment from the surface. Scale bar = 100 μm.

departure from the surface. After testing different conditions of flow rate and of internal volumes above the crystal (40–100 μL) (data not shown), we concluded that a low flow of 12 μL/min and an internal volume of 100 μL are required to minimize the shear forces due to the cross-flow above the MCF-7 cell layer and to preserve this latter. In these conditions, the frequency (less than 1 Hz) and the dissipation (less than $0.2 \times 10^{-6}$) shifts were in the usual range of the background noise of the sensor system (Fig. 2.B). Cell morphology was not affected by the dynamic culture conditions tested during 4 h (Fig. 2.C). The observations were confirmed by counting the residual cell number on the protein coated-sensor before setting the crystal in the QCM-D chamber and after 6 h of flow at 12 μL/min (2 h of equilibration and 4 h of signal monitoring) (Fig. S3). No difference had been detected between these two observations times.

### 3.3. QCM-D signature for cell apoptosis induced by STS

In order to determine if a specific QCM-D signal variation in relation with the short-term cytoskeletal cellular changes due to apoptosis could be highlighted, we first recorded the frequency and dissipation signal changes in response to a high STS concentration (10 μM) (Fig. 3A) and analyzed these results by comparing them to living treated MCF-7 cell images and residual cell counts (Fig. 3B and Fig. S4). Very quickly upon addition of STS, we observed a single-phase QCM-D signal. The $\Delta f$ and $\Delta D$ curves exhibit a sharp increase and decrease respectively. A plateau is reached after 2 h30 of STS treatment and remains stable until the end of the experiment. The increase in $\Delta f$ implies that lesser mass was detected at the sensor surface and the decrease in $\Delta D$ indicates a loss in viscoelasticity within the signal penetration depth. All together, these results point out a cell loss within the volume sensed by the crystal oscillations. These explanations are supported by the direct observation of the live cells by polarized light microscopy. Fig. 3B clearly shows a decrease in the adherent cell population after 1 h and 2 h of STS treatment, in correlation with the sharp shift observed for $\Delta f$ and $\Delta D$ signals. Between 2 h and 4 h, the number of cells on the surface appears stabilized as well as the $\Delta f$ and $\Delta D$ signals. The size and the shape of the remaining cells did not seem to be modified drastically and we could not observe any cellular debris remaining on the sensor surface. By the counting of the residuals cell number, we determined that about 60% of the initial cell was lost after the 4 h of STS at 10 μM exposure (Fig. S4).

### 3.4. Early detection of the cell response to low STS concentrations

As an aim to demonstrate that QCM-D technology could bring a direct detection of the early morphological signs of an apoptosis process with higher sensitivity and in a shorter time than the other classical analytical techniques in cell biology, we lowered the STS concentration in a range of 10 nM to 1 μM within which we could not observe any visible difference in residual cell counts (Fig. S4). The $\Delta f$ and $\Delta D$ signal records for the lower STS concentration (10 nM) were displayed Fig. 4.A. We managed to detect narrow but reproducible $\Delta f$ and $\Delta D$ responses after 1 h30 of treatment. $\Delta f$ and $\Delta D$ behaved similarly to what we observed for 10 μM STS treatment (Fig. 3.A). The frequency shift reached 5 Hz after 4 h and the dissipation shift $-6.3 \times 10^{-6}$. The real time observation of the cell during the QCM-D acquisition (Fig. 4.B) showed that the MCF-7 cell population resist to a 4 h exposure to 10 nM STS, without visible cell material loss. As the STS concentration increased from 10 nM to 1 μM, the induction of the dissipation response is faster and its magnitude greater, almost proportionately (Fig. 5). The time lapse required for the induction of the dissipation decrease is also inversely proportional to the STS concentration. Unlike the $\Delta D$ response, at low STS dose (10 nM to 1 μM), the all $\Delta f$ responses remained fairly similar among the low STS doses and did not exceed 6 Hz (data not shown). There is no clear dose dependency. In this concentration range, any modification of the adhering cell population could be observed (Fig. S5).

### 3.5. Effect of STS on the MCF-7 cell morphology

The morphological changes induced by STS treatment were further analyzed by scanning electron microscopy (Fig. 6). For this observation, the cells were subjected to the same conditions than for QCM-D measurements, except that, at this end of the QCM-D

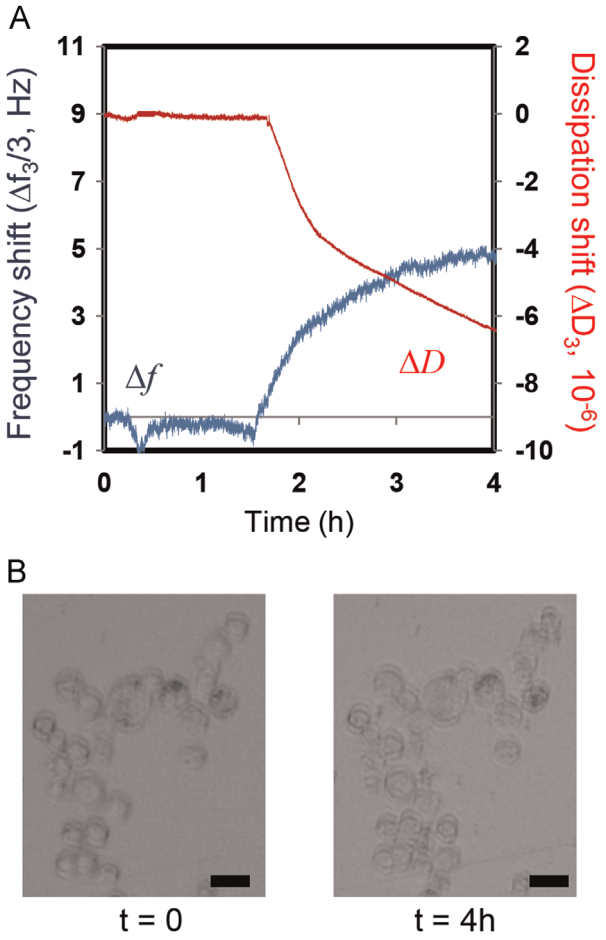


**Fig. 4.** (A) Simultaneously recorded $\Delta f$ and $\Delta D$ responses of MCF-7 cells exposed as a function of time in the presence of a continuous flow of 10 nM of STS. After 2 h of equilibration in the QCM-D chamber, the MCF-7 cells were exposed during 4 h to medium containing STS at a flow rate of 12 μL/min at 37 °C. (B) Live images of the MCF-7 cells on the sensor surface mounted in the QCM-D chamber at the beginning (left) and at the end (right) of these 4 h of monitoring. Scale bar = 10 μm.

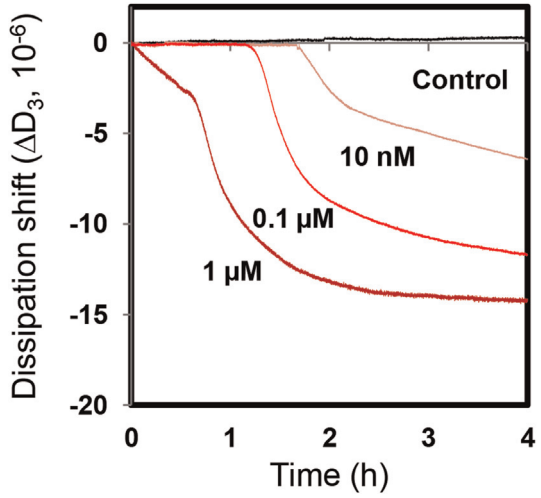


**Fig. 5.** $\Delta D$ (3rd overtone) responses induced by the exposure of MCF-7 cells to a continuous flow (12 μL/min) of STS solution in medium at the following concentrations: 0 μM, 10 nM, 0.1 μM and 1 μM during 4 h. The control (0 μM) was realized with a medium flow containing DMSO at the same concentration as a 10 μM STS solution.

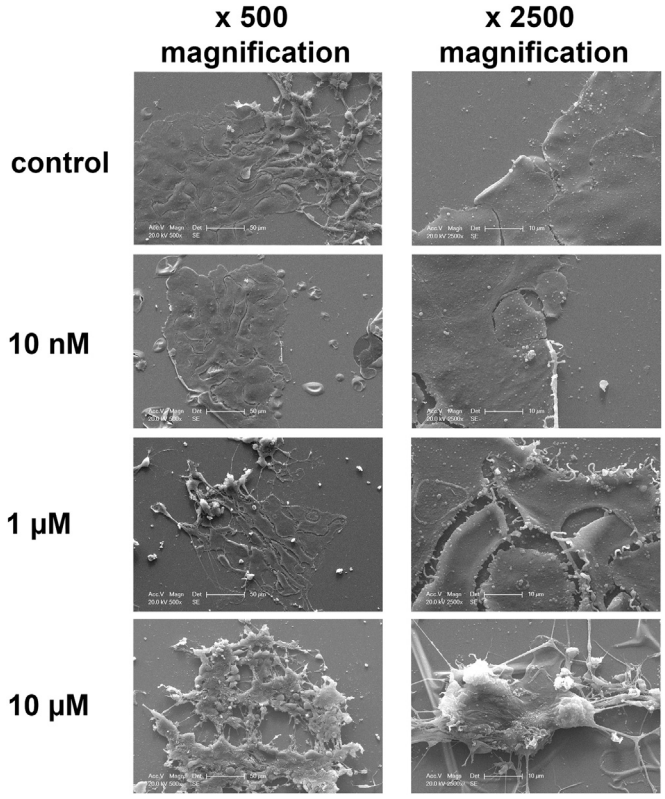


**Fig. 6.** Morphology of MCF-7 cells exposed to a continuous flow (12 μL/min) of different STS concentrations during 4 h. The control (0 μM) was realized with a medium flow containing DMSO at the same concentration as a 10 μM STS solution. Cells were examined using scanning electron microscopy.

monitoring, the residual cells were not trypsinized for counting but fixed and coated with gold for microscopy observations. Control MCF-7 cells exposed to a continuous flow (12 μL/min) were well-spread on gold coated surface with strong cell-cell contacts usually observed for these epithelial cells. Cell treatment with 10 nM STS did not alter cell morphology. With 1 μM STS, morphological changes appeared: some cells were less spread on the surface and cell junctions were less present. With 10 μM STS, MCF-7 cell morphology was deeply altered: cells remained attached on the surface only by few filamentous extensions and cell outlines were disturbed. We could clearly observe a rounding-up of the cells.

## 4. Discussion

In this present work, we aimed to demonstrate that the QCM-D interfacial sensor technology may bring a new way of detecting cell morphological changes due to programmed death. This technology is based on direct detection of changes in resonant oscillation parameters that are caused by mass or viscoelasticity modifications at a piezoelectric crystal interface. In our study, we intended to establish that this microbalance device could be employed to probe in real time early changes in the global cell adhesion in response to the apoptosis induction by anticancer drug. Indeed the shear wave penetration depth for the 3rd overtone for a 5 MHz crystal (138 nm in pure water at 25 °C) corresponds to the thickness of the interface between a cell and its substrate, *i.e.* the basal region of the cell, which is in the range of 100 nm (Bandey et al., 1999; Le Guillou–Buffello et al., 2011; Tymchenko et al., 2012). Moreover one of the great advantages of the QCM-D technology is that, once the cells are placed in the

QCM-D chamber, no more handling is required. This ensures the preservation of the complete cell integrity during the monitoring of their response to the drug (Fig. 2). We demonstrated that the cell adhesion to the sensing surface was not affected by the sensing surface, the medium flow or the oscillations of the crystal within the 6 h of the assay. This result is consistent with the conclusion of the work done by Heitmann and Wegener (2007). These authors have already demonstrated that shear oscillation amplitude at the driving voltage of 1 V, that we employed, is not high enough to displace attached cells from the surface and could be considered as non-invasive (Heitmann and Wegener, 2007).

In order to determine if QCM-D can be applied to characterize the cancer cell sensitivity to drugs in a very short time, we exposed human breast cancer cells, MFC-7, grown on FBS-protein-coated gold crystals to various concentrations of STS. We found a special interest in using the apoptosis inducer STS because the morphological changes resulting from its action are well representative of the general apoptosis consequences on cell adhesion. Apoptosis is morphologically characterized by rounding-up of the cell with reduction of the cellular volume (Bunel et al., 2014; Vanden Berghe et al., 2013). The STS treatment on MCF-7 cells leads to caspases 6 and 7 activation, proteases known to induce cytoskeleton proteins, such as actin, keratin, *etc*., cleavage and, as a consequence, leads to cell shrinkage and de-adhesion from the surface (Mooney et al., 2002). This makes it an ideal drug model for illustrating the QCM-D potentialities. Fig. 6 illustrates the impact on cell adhesion properties of STS at high concentrations. We would also like to stress upon the fact that the signaling pathways involved in the STS effect are really complex. This last point highlights the interests of finding an alternative method that could easily detect a global short-term cell response without the need to track down a precise signaling pathway perturbation.

The early detection of the first cell events related to an apoptosis process remains challenging. To have a better idea of the time scale required to detect early apoptosis signs with the detection methods usually employed, we performed Annexin V apoptosis detection assay on MCF-7 treated by STS during 4 h and 24 h (Figs. 1 and S2). This method is based on the observation that soon after initiating apoptosis, cells translocate the membrane phosphatidylserine from the inner face of the plasma membrane to the cell surface. This assay allows one of the earliest detection of apoptosis process (Martin et al., 1995). However, phosphatidylserine externalization was not revealed when cells were treated with high STS concentration for 4 h. A longer treatment (24 h) with STS was required to detect the phosphatidylserine flipping in MCF-7 cells. QCM-D would be a very interest complement to such analyses if a detection of the early cell responses to STS could be provided in only few hours. We decided to investigate if cell-substrate contact modifications due to apoptosis could be significantly detected within 4 h of STS treatment.

The QCM-D signal variations were recorded during the cell exposure to different concentration of STS from 10 nM to 10 μM. For all STS doses tested, the frequency and dissipation shifts display the same behavior with an increase in frequency and a decrease in dissipation (Figs. 3, 4 and 5). These frequency and dissipation shifts reflect in real time changes in cell attachment and/or in the viscoelastic properties of the attached cells in terms of coupled mass or viscoelastic properties (Chen et al., 2012). We could distinguish two levels of cell responses depending of the STS concentration. A first level for high STS concentrations ( $\geq 1$ μM) for which the QCM-D signal shifts could be directly correlated to observable cell morphological changes and second level for low STS concentration ( $< 1$ μM) which for any morphological impact (Fig. 6) nor phosphatidylserine flipping (Fig. 1) could be detected.

The first level of response would help us to correlate the general QCM-D signature obtained when cells are exposed to STS with the cell morphological changes occurring in the basal cell region. The Fig. 6 clearly shows that the effect of high STS dose (10 μM) on the MCF-7 cells is a rounding up and detachment from the sensor surface. This observation is reinforced by the loss of 40% of the initial cell number (Figs. 3 and S4) In term of QCM-D signal, this STS effect is reflected in a progressive loss of the detected mass and viscoelasticity by the quartz sensor within the sensing volume which leads to a frequency increase and a dissipation decrease respectively. Once detached from the crystal, the majority of the cells or of the cellular debris may get carried away by the flow, as no big apoptotic bodies could be observed by microscopy (Figs. 3.B. and 6). The same frequency and dissipation evolution has been also described for cell rounding induced by other cytomorphic agents, such as bovine aortic endothelial cells treated by lipopolysaccharides (LPS) from *Escherichia coli* which cause cell rounding (Fatisson et al., 2011). The same $\Delta f$ and $\Delta D$ changes were also described for murine and human fibroblasts (NIH3T3 and HS 483.T cells) upon cytochalasin exposure, which induced deep retraction and rounding of the cells (Tymchenko et al., 2012). Finally, an increase in the $\Delta f$ value and a decrease in the motional resistance ($R$) value were also reported by Braunhut and collaborators using the QCM to evaluate the response of two human breast cancer cell lines (MCF-7 and MDA-MB-231) to a steady-state taxane treatment (Braunhut et al., 2005). The authors suggested that theses $\Delta f$ and $\Delta$R changes reflect the cell rounding and the loss of adhesion during the apoptotic process.

On the basis on these elements, the QCM-D signature obtained at low STS dose can be interpreted as a decrease in the strength of the cell adhesion. The significant decrease in dissipation even for STS concentration of 10 nM (Fig. 5) and the absence of visible morphological alterations (Fig. 6) illustrate the high sensitivity of the QCM-D technique. Contrary to high dose of STS for which a drastic frequency changes were observed, the frequency shift is very weak compared to the energy dissipation shift below the STS concentration threshold of 1 μM (Fig. 4A). The same amplitude lag between the frequency and the dissipation shift were also noticed for cytochalasin action on fibroblasts (Tymchenko et al., 2012) or for epidermal growth factor-induced cell de-adhesion (Chen et al., 2011, 2012). At low STS dose, the frequency and dissipation changes reflected the very first steps of the cell de-adhesion process. Chen and collaborators have demonstrated that the dissipation response is quantitatively related to the level of focal adhesions (Chen et al., 2012). These authors suggested that the loss of the oscillating energy might be related to frictional and viscous slips involving the focal adhesion and/or the actin stress fibers (Kollmannsberger and Fabry, 2009). This allows an explanation as to why the dissipation signal is highly sensitive to the alteration of these cytoskeletal elements and how QCM-D could provide an early detection of the initial steps of cell disassembly (Marx et al., 2001). Conversely, this early disassembly of the focal adhesion do not necessary implies a significant mass lost in the sensing volume, that explains the weak shift in frequency and its absence of specificity concerning the low STS concentration range. For these reasons, we recommend focusing on the dissipation parameter, which better reflects the time-dependent changes in cell adsorption properties on the sensing surface, even for dose of STS in the nM range.

## 5. Conclusion

In this study, we have demonstrated that the QCM-D sensing is able to provide a real time and reproducible detection of the first morphological changes occurring at the cell/sensor surface interface when the cells are treated with an apoptosis inducer molecule. By varying the staurosporine concentration, we have

detected different cell behavior levels in response to drug exposure. High STS dose induces a QCM-D signature characteristic of cell rounding and detachment from the sensing surface. At low STS concentrations, we showed that QCM-D was able to sense early cytoskeletal events associated with apoptosis, which are not by the classical analytical techniques in cell biology within 4 h. We concluded that the energy dissipation shift could be used to track the short-term MCF-7 responses to staurosporine.

Given these results, QCM-D appears as a powerful technique to investigate and quantify the responses of a small number of live cells to apoptosis-inducing chemicals in dynamic conditions and without requiring their handling or labeling during the assay. The real time monitoring allows a precise determination of the cell response time and its scale. This study offers a new display of the interesting use of the QCM-D sensor in biomedical research for fast and highly sensitive drug screening assays, regardless of their molecular mechanism of action.

## Acknowledgment

We thank the European Union (co-funding of analytical equipment under CPER 2007–2013 and FEDER) and the Conseil Régional de Picardie for financial support (BetOX project). We also thank F. Oudet and all his collaborators for their help and advices for live imaging management. We acknowledge Dr. AjmalMaghoo for critical reading of the manuscript.

## Appendix A. Supplementary material

Supplementary data associated with this article can be found in the online version at http://dx.doi.org/10.1016/j.bios.2014.09.065.

## References

Asphahani, F., Zhang, M., 2007. Analyst 132 (9), 835–841.
Archana, M., Yogesh, T.L., Kumaraswamy, K.L., 2014. Indian J. Cancer 50 (3), 274–283.
Bandey, H.L., Martin, S.J., Cernosek, R.W., Hillman, A.R., 1999. Anal. Chem. 71 (11), 2205–2214.
Braunhut, S.J., McIntosh, D., Vorotnikova, E., Zhou, T., Marx, K.A., 2005. Assay Drug Dev. Technol. 3 (1), 77–88.
Bunel, V., Ouedraogo, M., Nguyen, A.T., Stevigny, C., Duez, P., 2014. Planta Med., http://dx.doi.org/10.1055/s-0033-1360273.
Chen, J.Y., Li, M., Penn, L.S., Xi, J., 2011. Anal. Chem. 83 (8), 3141–3146.
Chen, J.Y., Shahid, A., Garcia, M.P., Penn, L.S., Xi, J., 2012. Biosens. Bioelectron. 38 (1), 375–381.
Cooper, M.A., Singleton, V.T., 2007. J. Mol. Recognit. 20 (3), 154–184.
Demchenko, A.P., 2012. Exp. Oncol 34 (3), 263–268.
Dixon, M.C., 2008. J. Biomol. Tech. 19 (3), 151–158.
Fatisson, J., Azari, F., Tufenkji, N., 2011. Biosens. Bioelectron. 26 (7), 3207–3212.
Galluzzi, L., Vitale, I., Abrams, J.M., Alnemri, E.S., Baehrecke, E.H., Blagosklonny, M. V., Dawson, T.M., Dawson, V.L., El-Deiry, W.S., Fulda, S., Gottlieb, E., Green, D.R., Hengartner, M.O., Kepp, O., Knight, R.A., Kumar, S., Lipton, S.A., Lu, X., Madeo, F., Malorni, W., Mehlen, P., Nuñez, G., Peter, M.E., Piacentini, M., Rubinsztein, D.C., Shi, Y., Simon, H.U., Vandenabeele, P., White, E., Yuan, J., Zhivotovsky, B., Melino, G., Kroemer, G., 2012. Cell Death Differ. 19 (1), 107–120.
Heitmann, V., Wegener, J., 2007. Anal. Chem. 79 (9), 3392–3400.
Kanazawa, K., Gordon, J.G., 1985. The oscillation frequency of a quartz resonator in contact with a liquid. Anal. Chim. Acta 175, 99–105.
Kepp, O., Galluzzi, L., Lipinski, M., Yuan, J., Kroemer, G., 2011. Nat Rev Drug Discov 10 (3), 221–237.
Kollmannsberger, P., Fabry, B., 2009. Soft Matter 5, 1771–1774.
Le Guillou-Buffello, D., Gindre, M., Johnson, P., Laugier, P., Migonney, V., 2011. Biotechnol. Bioeng. 108 (4), 947–962.
Marx, K.A., Zhou, T., Montrone, A., Schulze, H., Braunhut, S.J., 2001. Biosens. Bioelectron. 16, 773–782.
Martin, S.J., Reutelingsperger, C.P.M., McGahon, A.J., Rader, J.A., van Schie, R.C.A.A., LaFace, D.M., Green, D.R., 1995. J. Exp. Med. 185 (1545-1556).
Marx, K.A., Zhou, T., Montrone, A., McIntosh, D., Braunhut, S.J., 2007. Anal. Biochem. 361 (1), 77–92.
Mooney, L.M., Al-Sakkaf, K.A., Brown, B.L., Dobson, P.R., 2002. Br. J. Cancer 87 (8), 909–917.
Rossi, C., Briand, E., Parot, P., Odorico, M., Chopineau, J., 2007. J. Phys. Chem. B 111 (26), 7567–7576.
Saitakis, M., Gizeli, E., 2012. Cell Mol. Life Sci. 69 (3), 357–371.
Tamaoki, T., Nomoto, H., Takahashi, I., Kato, Y., Morimoto, M., Tomita, F., 1986. Biochem. Biophys. Res. Commun. 135 (2), 397–402.
Tymchenko, N., Nilebäck, E., Voinova, M.V., Gold, J., Kasemo, B., Svedhem, S., 2012. Biointerphases 7 (1–4), 43.
Vanden Berghe, T., Grootjans, S., Goossens, V., Dondelinger, Y., Krysko, D.V., Takahashi, N., Vandenabeele, P., 2013. Methods 61 (2), 117–129.
Vockenroth, I.K., Rossi, C., Shah, M.R., Köper, I., 2009. Biointerphases 4 (2), 19–26.
Watarai, E., Matsunoa, R., Konnob, T., Ishiharaa, I., Takaib, M., 2012. Sens. Actuators B 171-172, 1297–1302.
Wegener, J., Janshoff, A., Steinem, C., 2001. Cell Biochem. Biophys. 34 (1), 121–151.
Xue, L.Y., Chiu, S.M., Oleinick, N.L., 2003. Exp. Cell Res. 283 (2), 135–145.
Zhou, B., Xiao, X., Xu, L., Zhu, L., Tan, L., Tang, H., Zhang, Y., Xie, Q., Yao, S., 2012b. Talanta 88, 345–351.
Zhou, T., Marx, K.A., Dewilde, A.H., McIntosh, D., Braunhut, S.J., 2012a. Anal. Biochem. 421 (1), 164–171.
Zhou, Y., Zeng, Y., Huang, S., Xie, Q., Fu, Y., Tan, L., Ma, M., Yao, S., 2012c. Sens. Actuators B 173, 433–440.